ANALYSIS OF PINE TREE HEIGHT ESTIMATION USING FULL WAVEFORM LIDAR

H.J. Park[a], R. Turner[b], S. Lim[a], J. Trinder[a], and D. Moore[c]

[a] School of Surveying and Spatial Information Systems, The University of New South Wales, Sydney, NSW 2052, Australia, hj.park@unsw.edu.au, s.lim@unsw.edu.au, j.trinder@unsw.edu.au

[b] Department of Industry and Investment NSW, Australia, Russell.Turner@industry.nsw.gov.au

[c] Terranean Mapping Technologies, Fortitude Valley, QLD 4006, Australia, David.Moore@terranean.com.au

Abstract - Many researchers have attempted to model and analyse three dimensional tree shape using remote sensing techniques. Airborne laser scanning or lidar is especially valuable since it provides a cost-effective, versatile, operationally flexible and robust sampling tool for forest management. Airborne laser scanning is able to provide full waveform lidar data that has a potential use for precision forestry.

The aim of this study is to determine the accuracy of tree height measurement from full waveform lidar processing techniques and to compare with alternative height extraction methods. Full waveform lidar was acquired at different densities of more than 2 points/m^2, over a *Pinus radiata* plantation test area in New South Wales, Australia. We examine the effect on accuracy of canopy height for varying densities and pine trees of varying ages and growth. The differences between the outputs derived by the full waveform lidar are compared with traditional field survey techniques and ground-based Terrestrial Laser Scanners.

Keywords: Forest Management, Full Waveform Lidar, Terrestrial Laser Scanner, Field Surveying, Canopy Height

1. INTRODUCTION

Light detection and ranging (lidar), which is an active remote sensing technique, provides direct range measurements between the lidar sensor and topography, which together with data about the aircraft position and orientation, provide accurate elevations on features on the terrain surface. The forest applications of lidar are diverse. For example, lidar is used for forest parameter estimation (Andersen et al, 2005), for estimating the vertical structure of vegetation (Wagner *et al.*, 2008) and extraction of forest variables by canopy height distribution (Maltamo *et al.*, 2006). The Canopy Height Model (CHM) of a forest represents the difference between the top canopy surface and the underlying ground topography (Zhao *et al.*, 2009). Previous lidar systems have already proven efficient in measuring canopy height (Lefsky *et al.*, 1999), and vertical distribution of canopy material (Dubayah and Blair, 2000). Recently, full waveform lidar systems are claimed to be important new developments in lidar technology. This system has been promoted with an emphasis on its capability of recording the complete waveform of the backscattered signal echo (Mallet, 2009). Full waveform systems can potentially provide a better representation of the tree canopy density structure, compared to discrete return systems (Parrish, 2007).

In this paper, we are investigating how to improve pine tree height estimates using full waveform data with three different pulse rates (80 kHz, 200 kHz, and 400 kHz). Moreover, the outputs derived by the full waveform lidar are compared with traditional field survey techniques and ground-based terrestrial laser scanners (TLS). This analysis of individual tree height was undertaken on four different age classes planted in 2008, 2005, 1994, and 1969.

2. DATA ACQUISITION

2.1 Testing Area

The study area was located in Sunny Corner, New South Wales (NSW), Australia. The acquisition covered a small area of 2km × 0.7km within a larger 13,000 hectare estate. A blue box in Figure 1 shows the test area, and the airplane trajectories are superimposed on the map with red lines.

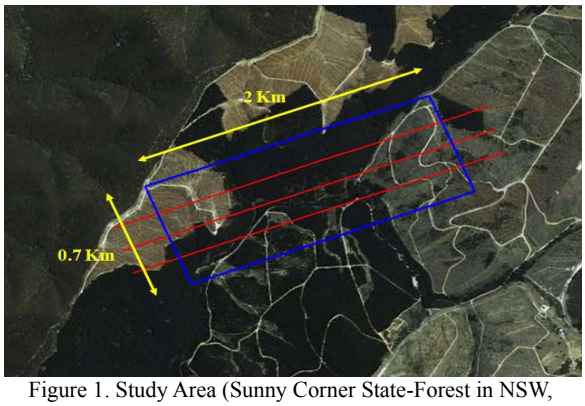

Figure 1. Study Area (Sunny Corner State-Forest in NSW, Australia)

2.2 Full Waveform Lidar

The lidar waveform data was collected on 11th September, 2010 using a Trimble's Harrier 68i system with RIEGL LMS-Q680i waveform sensor installed on a Beechcraft Bonanza A36. The lidar system specifications are listed in Table 1. Bathurst Airport, which is approximately 20km from the collection area, was used for the Global Position System (GPS) reference station. The reference coordinate system utilised in this experiment was the Map Grid of Australia (MGA) with the Geocentric Datum of Australia (GDA94) in Universal Transverse Mercator (UTM) Zone 55. The collection of lidar data was at 3 different pulse rates (80 kHz, 240 kHz, and 400 kHz), taken on 3 different strips i.e. three red lines in Figure 1. Flight speed was approximately 118 knots (1 knots = 0.514444m/s) during the survey (Max, 125knots).

Table 1. Full waveform lidar system specifications (RIEGL, 2010)

Lidar System Specifications	
Company / System	Trimble / Harrier 68i
Laser sensor	RIEGL LMS-Q680i
Beam deflection / Scan pattern	Pyramid. Polygon mirror / Parallel scan lines
Scan angle	Up to ± 30.0 degrees
Laser pulse rate (pulse repetition frequency)	Up to 400,000 Hz PRF
Minimum & Maximum Range	30 m / 1500 m (Approximately)
Laser wavelength / Intensity capture	1,550 nm / 16 bit per return amplitude
Spot diameter	50 cm @ 1,000 m
Pulse resolution	0.1m (wave form mode) pulse width resolution
Point accuracy (horizontal / vertical)	19 cm / 7 cm (1 sigma)

2.2 Terrestrial Laser Scanning Data and Field Surveying

Field surveys were performed to obtain reference data for a variety of pine trees located within the study area. These included Total Station (TS) to survey Ground Control Points (GCPs) that were visible in the lidar data, and Terrestrial Laser Scanning (TLS) for determining individual tree canopy heights. Figure 2 shows the location of TS and TLS stations. Red dots represent the GCPs (Ground Control Points) and blue circles show the locations of the reference tree samples using TLS with TS.

Figure 2. Location of TLS with TS in Testing Area

Nine GCPs were surveyed with a Leica GPS-1200 receiver. Each point was measured in the static mode with long observation sessions of more than 60 minutes as the baselines in this survey were less than 25 km long (from Bathurst & Lithgow).

Using the GCPs as a starting point, each tree location and height was surveyed with TS (Leica TCRP 1203). The TS was used in reflectorless mode to measure pine tree canopy height. Secondly, the TLS (Leica Scan Station C10) measured high-density point data for each sample tree. The field surveying observation did not compensate for variation in wind velocity or direction. The final reference data set contained 30 sample trees per age class making a total of 120 sample trees.

3. DATA PROCESSIGN

Full waveform lidar processing involves many steps with each requiring a variety of processing algorithms. The first stage is the waveform pulse signal processing, then sensor data deconvolution, geo-referencing with Position and Orientation System (POS) data, and data conversion to point clouds and extraction of tree canopy height. An algorithm for each processing stage was created, but commercial software was also occasionally used. The data processing scheme is illustrated in Figure 3.

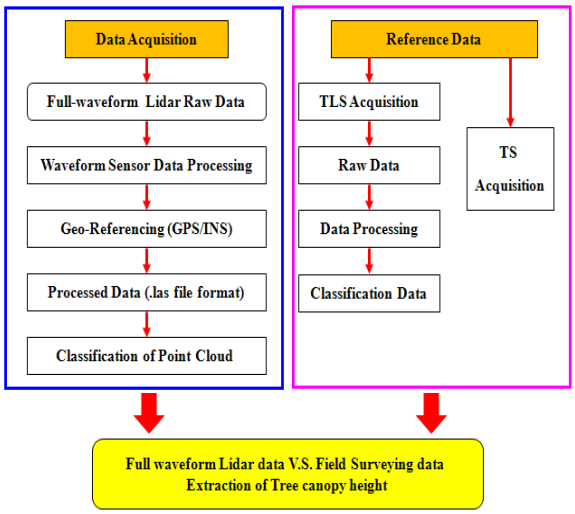

Figure 3. Flowchart of full waveform lidar with field surveying data processing

3.1 Waveform Signal Processing

Using deconvolution techniques, the cross-section profile may be derived if the system waveform is known. The full waveform lidar equation is derived from the fundamental radar equation and describes the return power as a function of the system's specifications i.e. receiver aperture diameter, distance to target and system transmission factor (Wagner *et al*, 2006).

$$P_r(t) = \sum_{i=1}^{n} \frac{D_r^2\, \eta_{sys}\, \eta_{atm}}{4\pi\, R_i^4\, \beta_i^2}\, S(t) * \sigma_i\,(R) \qquad (1)$$

where P_r is the received signal power $[w]$, S is the transmitted system waveform $[DN]$, D_r is diameter of receiver aperture $[m]$, R is range from sensor to target $[m]$, β is laser beam divergence $[rad]$, η_{sys} is system transmission factor $[-]$, η_{atm} is atmospheric transmission factor $[-]$, and σ is backscatter cross section $[m^2]$.

The returned backscattered power can be formulated in terms of the convolution between the system waveform $S(t)$ and cross section $\sigma(t)$ (Wagner *et al*, 2006). This can be described as:

$$P_r(t) = S(t) * \sigma(t). \qquad (2)$$

Each lidar waveform was modelled as a linear combination of Gaussian functions using Equation (3)

$$P_r\,(t) = \sum_{i=1}^{N} \hat{P}_i \exp\left\{-\frac{1}{2\sigma_i^2}(t - t_i)^2\right\} \qquad (3)$$

where t_i is the time taken for round-trip, σ_i is the standard deviation of the echo pulse, $\hat{P}_i$ is the amplitude of target i, and

N is the number of targets within the travel path of the laser pulse.

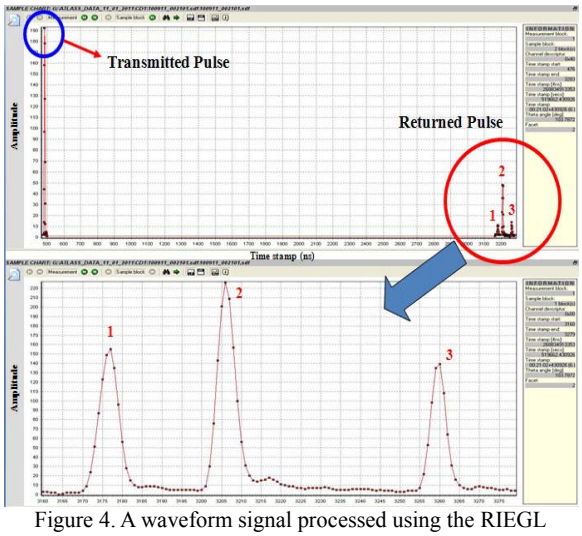

Figure 4. A waveform signal processed using the RIEGL software

Figure 4 shows examples of waveform signals displayed using commercial software (RIEGL, 2010). This processing used deconvolution techniques, the cross-section profile may be derived if the system waveform is known. In the upper plot of Figure 4, X and Y represent the time stamp and the amplitude, respectively. The blue-coloured circle represents the transmitted pulse data and the red-coloured circle, the return pulse data. The lower plot in Figure 4 illustrates the details of the recorded waveform based on the fitting of a Gaussian function (shown in the Figure 4 as a red-colour solid line).

3.2 Geo-Referencing

Geo-referencing was based on the matching of the GPS time with sensor single timestamps t. This processing used the GPS/IMU integration method with transformation matrix equations. In the processing, the waveform and sensor data are required as well as the post-processed position and orientation data, Inertial Measurement Unit (IMU) offsets, scanner angles and misalignment angles. The equation for the laser geo-location can be given in vector-matrix notation as follows (El-Sheimy, 2009):

$$r_i^m = r_s^m(t) + R_s^m(t)\, r_i^s \qquad (4)$$

where r_i^m is the position vector of an object i in the three-dimensional coordinate frame (latitude, longitude, and height), t is the epoch for measuring the distance d for i, $r_s^m(t)$ is the position of the scanner mirror (the origin of the laser scanner coordinate frame) in the mapping frame at the time of the laser shot, r_i^s is the 3 × 1 position vector of i, and α is the scanner angle in the laser sensor frame which is given as

$$r_i^s = \begin{pmatrix} d\sin\alpha \\ 0 \\ d\cos\alpha \end{pmatrix}. \qquad (5)$$

When geo-referencing the data, POS data from GPS/IMU system is used in conjunction with sensor data. We used a North-East-Down (NED) navigation frame and followed the counter-clockwise rotation (in a right handed system).

3.3 Data Processing Result

As a general result, a 3D point cloud is shown in Figure 5. Following the classification of the point clouds, the heights were colour coded, with red the highest points and blue the lowest in Figure 5a). Figure 5b) shows the classification of ground point data (pink colour) with non-ground point data (green colour). Each point data contains information of E, N, H and I (E: Easting, N: Northing, H: Height and I: Intensity of the return signal).

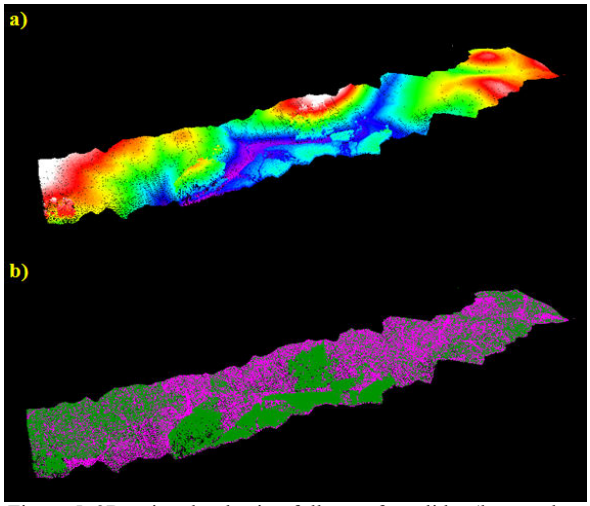

Figure 5. 3D point cloud using full waveform lidar (laser pulse rates: 80 kHz); a) elevation data, b) classification data

The total number of processed full waveform lidar points and the number of returns are illustrated in Table 2 for three different pulse rates of 80 kHz, 200 kHz, and 400 kHz respectively.

Table 2. Full waveform lidar data results

Full waveform lidar Point Cloud Data result			
Point Number	Sensor Pulse Rates		
	80 kHz	200 kHz	400 kHz
Return 1	2,733,695	7,249,953	13,945,629
Return 2	546,242	1,614,846	2,294,417
Return 3	283,856	741,307	675,416
Return 4	160,624	319,961	152,964
Return 5	85,698	115,040	24,063
Total Point	3,866,384	10,086,208	17,095,470

3.4 TLS Processing

In this study the post-processing of the 3D point clouds was performed with Leica's Cyclone 7.0. This software offers registration and geo-referencing of point clouds as well as multiple options for post-processing. The Root Mean Square Errors (RMSE) of the geo-referencing of all TLS data were 0.015m horizontally and 0.040m vertically.

After processing and georeferencing all datasets it is possible to compared full waveform lidar (80 kHz, 240 kHz, and 400 kHz), with TLS and TS data. Figure 6 shows the example of processed images.

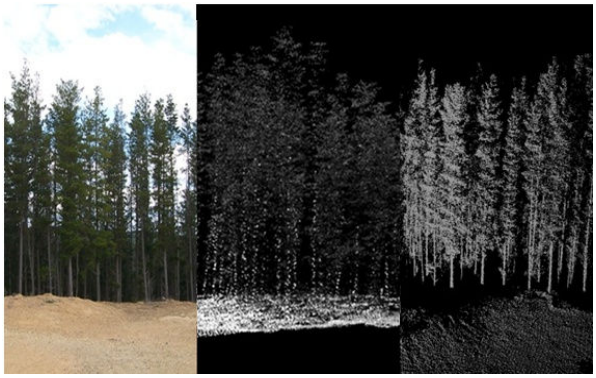

Figure 6. Image of tree v.s. full waveform lidar data (laser pulse rates: 400 kHz) v.s. TLS data in the study area (1969 age of trees)

4. ANALYSIS OF PINE TREE HEIGHT

Analysis of the data is still in progress but there are two issues that merit further discussion: one is the accuracy of pine tree canopy height with different pulse rates, compared with traditional field survey techniques and TLS data. The reference data was based on TLS measurements which provide a much higher resolution than the conventional field surveying methods.

Tree Ages / Equipments	2008 (30 Sample Trees)		2005 (30 Sample Trees)		1994 (30 Sample Trees)		1969 (30 Sample Trees)	
	Average (m)	RMSE (m)	Average (m)	RMSE (m)	Average (m)	RMSE (m)	Average (m)	RMSE (m)
Total Station	0.196	0.251	0.259	0.287	0.250	0.281	0.304	0.311
Lidar Height (80 kHz)	1.001	1.051	1.491	1.558	0.813	0.949	0.646	0.727
Lidar Height (200 kHz)	0.849	0.890	1.108	1.148	0.525	0.614	0.307	0.362
Lidar Height (400 kHz)	0.662	0.689	1.018	1.063	0.545	0.601	0.248	0.303

Figure 7. Comparison of TS and full waveform lidar derived pine tree heights with the TLS reference data

Figure 7 shows the differences in TLS derived pine tree heights with those derived from TS and full waveform lidar data.

5. CONCLUSIONS

This study investigated an innovative approach to forest inventory for tree y height estimation, using full waveform sensor signal data together with TLS data. We examined the effect on height accuracy of varying lidar sampling point densities for pine trees of varying ages and crown sizes. Results showed the average height error was 0.304m (derived from the TS), 0.646m (for 80kHz lidar data), 0.307m (for 240kHz lidar data), and 0.248m (for 400kHz lidar data), respectively. This suggests that the highest density of airborne lidar data provided the best estimate of individual tree heights. . We hope that these results may assist in planning future airborne lidar missions in softwood plantations.

REFERENCES

1. Andresen, H.-E., Mcgaughey, R., Reutebuch, S., 2005. Estimating forest canopy fuel parameters using LIDAR data. Remote Sensing of Environment **94** (6) pp. 441-449.
2. Dubayah, R. and Blair. J., 2000. Lidar Remote Sensing for Forestry Applications, Journal of Forestry **98** (6) pp 44–46.
3. EI-Sheimy, N. 2009, Georeferencing Component of LiDAR Systems, *In:* Shan, J. & Toth, C. K. (eds.) *Topographic Laser Ranging and Scanning: Principles and Processing*, NorthWestern: CRC Press. pp 210–213.
4. Lefsky, M.A., Cohen, W.B., Acker, S.A., Parker, G.G., Spies, T.A. and Harding, D., 1999. Lidar remote sensing of the canopy structure and biophysical properties of Douglas-fir western hemlock forests. *Remote Sensing of Environment*, **70**(3) pp. 339-361.
5. Mallet, C. and Bretar, F. 2009, Full-waveform topographic lidar: State-of-the-art, *ISPRS Journal of Photogrammetry and Remote Sensing,* **64** pp. 1-16.
6. Maltamo, M., Malinen, J., Packalen, P., Suvanto, A., And Kangas, J., 2006, Nonparametric estimation of stem volume using airborne laser scanning, aerial photography, and stand-register data. Canadian Journal of Forest Research, **36** pp. 426-436.
7. Parrish, C. E. 2007, Exploiting full-waveform lidar data and multiresolution wavelet analysis for vertical object detection and recognition, *Geoscience and Remote Sensing Symposium, 2007 IEEE International; Barcelona,Spain*.
8. RIEGL, 2010, *Laser Measurement Systems*, http://www.riegl.com visited on 11/10/2010.
9. Wagner, W., Ullrich, A., Ducic, V., Melzer, T. and Studnicka, N. 2006, Gaussian decomposition and calibration of a novel small-footprint full-waveform digitising airborne laser scanner, *ISPRS Journal of Photogrammetry and Remote Sensing,* **60**, 100-112.
10. Wagner, W., Hollaus, M., Briese, C., and Ducic, V., 2008. 3D vegetation mapping using small footprint full-waveform airborne laser scanners. International Journal of Remote Sensing **29** (5) pp.1433-1452.
11. Zhao, K., Popescu, S., Nelson, R., 2009, 'Lidar remote sensing of forest biomass: A scale-invariant estimation approach using airborne lasers', *Remote Sensing of Environment*, **113** (1) pp.182-196.

ACKNOWLEDGEMENTS

The authors would like to thank Terranean Mapping Technologies for providing full waveform lidar data, Hard & Forester Surveyors for providing TLS data for this research, and Forests NSW for assistance and authorisation to utilise the plantation study area.